Lithologic Discontinuity Assessment in Soils via Portable X-ray Fluorescence Spectrometry and Visible Near-Infrared Diffuse Reflectance Spectroscopy

David C. Weindorf*
Dep. of Plant and Soil Science
Texas Tech Univ.
Lubbock, TX 79409

Somsubhra Chakraborty
Uttar Banga Krishi Viswavidyalaya
Cooch Behar
India

**Abdalsamad Abdalsatar
Ali Aldabaa**
Desert Research Center
Cairo
Egypt

Laura Paulette
Univ. de Ştiinţe Agricole şi
Medicină Veterinară
Cluj-Napoca
Romania

**Giuseppe Corti
Stefania Cocco**
Dipartimento di Scienze Agrarie,
Alimentari ed Ambientali
Univ. Politecnica Delle Marche
Ancona
Italy

Erika Michéli
Szent István Univ.
Gödöllő
Hungary

Dandan Wang
Nanjing Univ. of Information
Science & Technology
Nanjing
China

Bin Li
Louisiana State Univ.
Baton Rouge, LA 70803

Titus Man
Babeş-Bolyai Univ.
Cluj-Napoca
Romania

**Aakriti Sharma
Taylor Person**
Dep. of Plant and Soil Science
Texas Tech Univ.
Lubbock, TX 79409

Lithologic discontinuity identification can be arduous and erroneous in instances where distinct morphological differences between parent materials are absent. Often, investigators must wait for laboratory data to help differentiate parent materials via physicochemical properties. This study used visible near-infrared diffuse reflectance spectroscopy (VisNIR DRS) and portable X-ray fluorescence (PXRF) spectrometry for establishing parent material differentia more quickly. Ten pedons containing 135 samples were scanned in situ in the United States, Italy, and Hungary, morphologically described by trained pedologists, then sampled for standard laboratory characterization. Compared with laboratory data and/or morphologically described discontinuities, PXRF data were associated with large, abrupt changes in standardized PXRF differences of elements (DEs), noted in data plots as DE maxima and minima—areas of likely discontinuity. Standardized VisNIR DRS calculated differences (CDs) in reflectance spectra (350–2500 nm) were also associated with discontinuities based on CD reflectance maxima and minima. Notably within both types of data plots, lithologic discontinuities were not well captured by the proximal sensors when CD or DE values fell in the data plot midsection (i.e., not at maxima or minima within the data plots). Across the pedons evaluated, PXRF was more useful for detecting discontinuities than VisNIR DRS. Summarily, PXRF showed good alignment with morphologically established discontinuities in eight out of 10 pedons, while VisNIR DRS showed good alignment in only five pedons. Both PXRF and VisNIR DRS provided useful information for lithologic discontinuity recognition, especially in soils with nondescript morphology.

Abbreviations: CD, calculated difference; DE, difference of elements; EC, electrical conductivity; LD, lithologic discontinuity; PCA, principal component analysis; PXRF, portable X-ray fluorescence; SOM, soil organic matter; VisNIR DRS, visible near-infrared diffuse reflectance spectroscopy.

Lithologic discontinuities (LDs) are defined as zones within the pedo-stratigraphic column representing a change in lithology, sediment type, or parent material (Soil Science Society of America, 2014). The formation of LDs can be by geologic depositional processes before pedogenesis, deposition (e.g., new sediment addition) during soil formation, weathering, vertical or lateral translocations, or bioturbation (Phillips and Lorz, 2008; Schaetzl and Thompson, 2015). In some cases, LDs are marked by changes in soil texture, coarse fragment content, soil organic C, or other physicochemical parameters (Schaetzl, 1998). If the aforementioned features are present, morphological establishment of the LDs is relatively straightforward to the trained pedologist. However, many instances exist where LDs are nondescript and cannot be easily surmised. In fact, many pedologists concede that LDs are often difficult to recognize in the field due to a lack of clear morphological expres-

sion (e.g., Price et al., 1975; Soil Survey Staff, 1993). For example, in northeastern Wisconsin and the Upper Peninsula of Michigan, Schaetzl and Luehmann (2013) noted that pedoturbation could effectively mix loess with the underlying sandy glacial sediment in zones up to 50 cm thick. This emphasizes the fact that many LDs have boundaries that are not abrupt. Thus, pedologists are left to field identify suspected LDs using data they can obtain from the soil profile, collect samples, and await the results of physicochemical laboratory analyses in support of their suppositions. Given the depth and breadth of experience of most pedologists, their field conclusions on soil physicochemical properties, soil profile pedogenesis, and suspected LDs are remarkably accurate; yet at times even such talented professionals find themselves in need of confirmatory laboratory analyses. Such laboratory data typically involve the skeletal, immobile fraction of soils. Grain size analysis may be evaluated independently (e.g., sand, silt, and clay) or as ratios of sand/silt, coarse sand/fine gravel fractions, quartz/feldspar ratios, and elemental composition or mineralogy (Foss and Rust, 1968; Raad and Protz, 1971; Schaetzl, 1998; Price et al., 1975; Habecker et al., 1990). While these techniques are generally effective, they require laboratory analysis without the ability to provide pedologists with the necessary data while evaluating pedons in the field. However, the advent of field-portable, proximal sensors (e.g., portable X-ray fluorescence [PXRF] spectrometry and visible near-infrared diffuse reflectance spectroscopy [VisNIR DRS]) offers new means of investigation in situ and provides field soil scientists with on-site quantitative data (McLaren et al., 2012; Hartemink and Minasny, 2014). Importantly, these approaches offer advantages over traditional laboratory analyses such as nondestruction, speed, and low operating cost.

Portable X-ray fluorescence utilizes fluorescent emission spectra given off by elements bombarded by low-power X-rays (10–40 kV). The wavelength (energy) of the emitted spectra are characteristic of unique elements present in a sample, whereas emission intensity gives an indication of elemental abundance. Conversely, VisNIR DRS involves the use of reflected light in the 350- to 2500-nm range. Reflectance spectra are parsed into discreet intervals (e.g., 2–10 nm) to construct reflectance profiles, which are then statistically compared with other quantitative soil parameter data. Various soil parameters are uniquely associated with combinations of specific reflectance spectra (Chakraborty et al., 2010). Comprehensive overviews of PXRF, VisNIR DRS, and their potential synthesis in soil analyses have been offered by Weindorf et al. (2014) and Horta et al. (2015).

Previously, PXRF and VisNIR DRS have been independently used to successfully predict a wide range of soil physicochemical properties, including organic C (Morgan et al., 2009; Chakraborty et al., 2013), gypsum content (Weindorf et al., 2009, 2013a), salinity (Swanhart et al., 2014), pH (Sharma et al., 2014), texture (Zhu et al., 2011), cation exchange capacity (Sharma et al., 2015), diagnostic subsurface horizons and features (Weindorf et al., 2012c), moisture (Zhu et al., 2010), and organic and inorganic pollutants (Weindorf et al., 2012a, 2013b; Chakraborty et al., 2010; Paulette et al., 2015). Most im-

portantly, Weindorf et al. (2012b) showed that PXRF could be used for enhanced soil horizonation whereby horizons could be differentiated using elemental data from PXRF in soil profiles where morphological differentia were unremarkable. Applied to the present study, VisNIR DRS models have another advantage in that they should be able to better detect irregular decreases in organic C content with depth—an established approach for recognizing buried soils and potential discontinuities.

Although each of these techniques has successfully predicted soil physicochemical properties independently, the latest research has investigated the synthesis of data from these two approaches for enhanced predictive model performance. For example, a fused PXRF–VisNIR DRS approach was used to provide optimized predictive models of soil salinity in playas of West Texas (Aldabaa et al., 2015), total C and total N in soils (Wang et al., 2015), and hydrocarbon quantification in contaminated soils (Chakraborty et al., 2015). In all three studies, performance of the fused PXRF–VisNIR DRS predictive models outperformed the models that utilized only a singular proximal sensor.

Given the success of VisNIR DRS and PXRF at predicting numerous soil physicochemical properties, evaluation of their use for field identification of LDs in soils appears timely. If proven successful, it would offer pedologists a rapid, quantifiable means of determining LDs in situ, especially in nondescript soils where no morphological differences present themselves and in instances where mixing between two parent materials produces a gradual or diffuse boundary between materials. As such, the objective of this research was to compare soil LDs established by traditional morphological field description with physicochemical data produced through standard laboratory characterization with that of proximally sensed PXRF and VisNIR DRS data. Our goal was to relate the data sets to determine the effectiveness of PXRF–VisNIR DRS in establishing LD boundaries. We hypothesized that both PXRF and VisNIR DRS would successfully differentiate parent materials in situ, allowing LD identification.

MATERIALS AND METHODS
General Occurrence and Features

In an effort to test the effectiveness of this approach on a wide variety of LDs, samples of 10 pedons were collected in West Texas (TX) (*n* = 5), Italy (IT) (*n* = 2), and Hungary (HU) (*n* = 3). Collectively, the pedons consisted of 135 samples collected at fixed depths. The coordinates of samples from 10 locations and their taxonomic classification are given in Table 1.

In Texas, sampling was conducted in Cochran and Terry counties in Major Land Resource Area 77C: Southern High Plains—Southern Part. The area is found on an expansive level plateau characterized by an ustic moisture regime (405–560 mm of precipitation) that borders on aridic, with a thermic temperature regime (13–17°C) (Soil Survey Staff, 2006). Soils of the area are largely derived from aeolian deposits of the Blackwater Draw Formation of Pleistocene age, with some alluvium and lacustrine sediments associated with shallow playas and ephemeral streams (Soil Survey Staff, 2006).

In Italy, soils were sampled at two different sites: Valleremita and Gallignano. The former developed on layers of detritus known as grèzes litées, which formed during the last glaciation (Würm) by slopes composed of layers of well-sorted angular stones originated by frost shattering and displaced by snowmelt. Along the central part of the Apennines chain, large areas are covered by this type of layered deposits made of shattered limestone fragments of different dimensions immersed in a silty matrix. The soil moisture regime is udic (945 mm of precipitation) and the temperature regime is mesic (12.6°C) (Soil Survey Staff, 2010). Gallignano soils developed from finely ground marine sediments that consisted of lithologic units with pelitic-arenaceous or arenaceous-pelitic composition, all containing carbonates. The soil is characterized by an ustic moisture regime (780 mm) that borders on udic and a mesic temperature regime (13.6°C) (Soil Survey Staff, 2010).

In Hungary, all sampled soils were located in north-central Hungary and developed from Pleistocene loess. The composition of the loess varies in the Carpathian Basin according to the major distance sources and local sources of aeolian sediments (Horváth, 2001). Pedon HU-2 was located close to the pediment of the Matra Hills, which served as the local source of fine particles from weathered andesitic material (Horváth et al., 2005). Pedons HU-4 and HU-5 were influenced by local coarser sandy sources of older Tertiary deposits eroded to the surface (Stefanovits, 1963). Profile HU-2 developed in a stable plateau position under natural grass vegetation. Pedons HU-4 and HU-5 experienced more erosion and translocations of surface materials during the late Pleistocene and the Holocene. The natural vegetation in the Holocene was forest. The annual precipitation at the sites is between 450 and 550 mm, the moisture and temperature regimes being ustic and mesic, respectively (Michéli et al., 2006).

Pedons from Texas were collected utilizing a hydraulic probe (Giddings Probe). Pedons from Italy were collected from exposed road cuts or erosional escarpments. In Hungary, pedons were sampled from soil pits opened with a backhoe. At each location, the evaluated area (of both the excavation walls and cores) was scraped clean with a knife, then scanned with proximal sensors in 10-cm increments (e.g., 0–10, 10–20 cm, and so on) in situ in a manner consistent with Weindorf et al. (2012b). Texas field scanning included both PXRF and VisNIR DRS, while Italian and Hungarian field scanning used only PXRF due to logistical limitations relative to international transport of equipment. After scanning, morphological field evaluation (Schoeneberger et al., 2002) was used to determine the suspected depth of LDs. Field notes were made and profiles were photographed (Fig. 1). Soils were sampled in 10-cm increments to coincide with the aforementioned proximal scanning depths, thus avoiding any bias associated with morphologically established LD boundaries. Samples were sealed in plastic bags and sent to the Texas Tech University pedology laboratory for further characterization. Samples collected in Italy and Hungary were dried and crushed before shipment to Texas Tech University.

Table 1. Geographic coordinates and taxonomic classification of soils evaluated for lithologic discontinuities in Texas, Italy, and Hungary.

Site	Latitude	Longitude	Taxonomic classification†
TX-1	33.68 N	102.94 W	Ustic Epiaquert
TX-2	33.69 N	103.02 W	Aridic Paleustalf
TX-3	33.02 N	102.35 W	Aridic Ustifluvent
TX-4	33.15 N	102.11 W	Aeric Halaquept/ Torrifluventic Haplustept
TX-5	33.26 N	102.20 W	Aridic Ustifluvent
IT-2 (Valleremita)	43.29 N	12.87 E	Eutric Humustept
IT-3 (Gallignano)	43.56 N	13.43 E	Typic Eutrudept
HU-2	47.69 N	19.62 E	Typic Haplustoll
HU-4	47.59 N	19.37 E	Ultic Haplustalf
HU-5	47.59 N	19.37 E	Ultic Haplustalf

† Soil Survey Staff, 2010, 2015.

Soil Characterization

In the laboratory, all dried samples were ground to pass a 2-mm sieve, then subjected to standard soil characterization. Particle-size analysis was accomplished via hydrometer, with clay readings at 1440 min using a Model 152-H hydrometer and the method of Gee and Bauder (1986) and sand determined gravimetrically after wet sieving at 53 μm. Soil pH and electrical con-
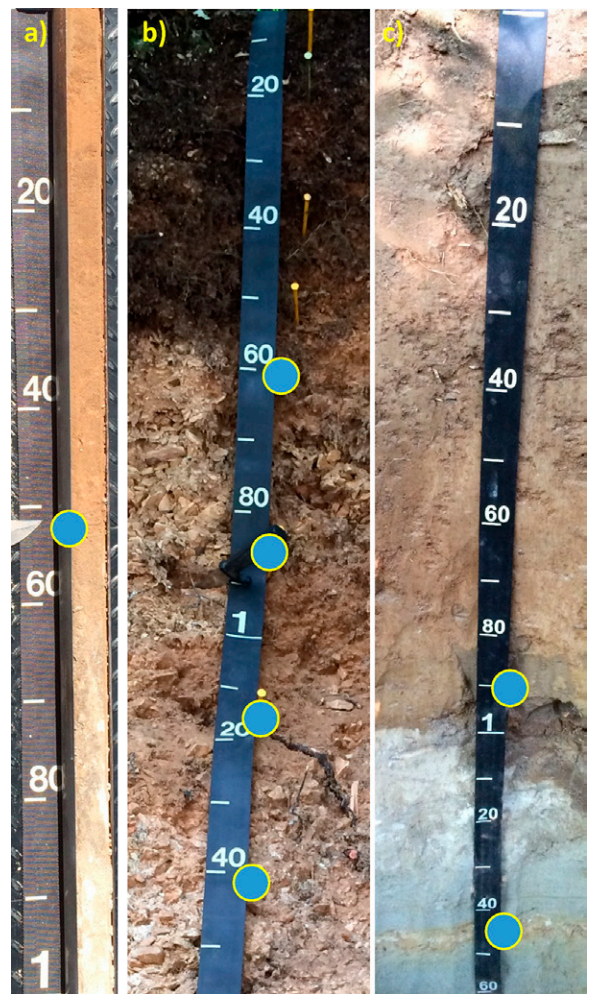
Fig. 1. Photographs of sampled pedons in (a) Texas (TX-5), (b) Italy (IT-2), and (c) Hungary (HU-4). Field-suspected lithologic discontinuities are marked with a dot. Depth measurements on tape measures are in centimeters.

ductivity (EC) were determined via saturated paste after 24-h equilibration using an Accumet XL20 pH/conductivity meter (Salinity Laboratory Staff, 1954; Soil Survey Staff, 2004). Soil organic matter (SOM) was determined according to Nelson and Sommers (1996) after 8 h of ashing at 400°C to minimize dehydroxilation of the mineral soil. Calcium carbonate content was determined on the TX pedon samples via a pressure calcimeter (Sherrod et al., 2002). Pedons from Italy and Hungary were subjected to total C and total N analyses using Dumas method high-temperature combustion on a LECO TruSpec CN analyzer (Soil Survey Staff, 2014a).

Portable X-ray Fluorescence Spectrometry

Each sample was subjected to PXRF scanning with a DP-6000 Delta Premium PXRF (Olympus) with deference to USEPA Method 6200 (USEPA, 2007). The instrument features an Rh X-ray tube operated at 10 to 40 kV with an integrated large-area silicon drift detector (165 eV). Before scanning, the instrument was calibrated with a 316 alloy calibration clip tightly fitted over the aperture. Scanning was conducted in Soil Mode (three beam), which is capable of detecting the following suite of elements: V, Cr, Fe, Co, Ni, Cu, Zn, Hg, As, Se, Pb, Rb, Sr, Zr, Mo, Ag, Cd, Sn, Sb, Ti, Mn, P, S, Cl, K, and Ca; each sample was then scanned a second time using Geochem Mode (two beam) to measure Mg. Scanning in Soil and Geochem modes was conducted at 30 s per beam. Geochem and Soil mode scans were both done in duplicate, with the spectrometer repositioned between each scan. Data were then averaged between scans to obtain a mean of elemental data for each soil sample evaluated. The performance of the PXRF was checked via scanning NIST-certified soil samples; results for one of those (NIST 2710a– Montana I soil) were (PXRF reported/NIST certified [recovery]: K, 24,376/21,700 mg kg^{-1} [1.12]; Ca, 8998/9640 mg kg^{-1} [0.93]; Ti, 3415/3110 mg kg^{-1} [1.10]; Mn, 2189/2140 mg kg^{-1} [1.02]; Fe, 47,055/43,200 mg kg^{-1} [1.09]; Cu, 3346/3420 mg kg^{-1} [0.98]; Zn, 4236/4180 mg kg^{-1} [1.01]; As, 1538/1540 mg kg^{-1} [1.00]; Sr, 259/255 mg kg^{-1} [1.02]; Ba, 691/792 mg kg^{-1} [0.87]; Pb, 5476/5520 mg kg^{-1} [0.99]. Given that Weindorf et al. (2012b) reported that PXRF scans conducted under field, laboratory, or monolith conditions achieved almost the same results and the influence of moisture was <20% on PXRF data is nominal (Melquiades et al., 2011; Piorek, 1998), only field-moist scans were used for this study. All field-moist samples evaluated as part of this study were, in fact, quite dry.

Visible Near-Infrared Diffuse Reflectance Spectroscopy and Spectral Pretreatment

All soil samples were scanned using a PSR-3500 portable VisNIR DRS spectroradiometer (Spectral Evolution, USA) with a spectral range of 350 to 2500 nm. The spectroradiometer had a 2-nm sampling interval and a spectral resolution of 3.5, 10, and 7 nm from 350 to 1000, 1500, and 2100 nm, respectively. Scanning was accomplished using a contact probe with a

5 W built-in halogen light source. Samples were dried, ground, and scanned at room temperature in the laboratory, evenly distributed in an opaque polypropylene sample holder and scanned from the top with the contact probe connected to the PSR-3500 with a metal-clad fiber optic cable. Full contact with the sample was guaranteed to avoid outside interference. Each sample was scanned four times, rotating the sample 90° between scans. The four scans were then used to obtain an average spectral curve. Each individual scan was an average of 10 internal scans over 1.5 s. White referencing of the detector (after each sample) was accomplished using a 12.7- by 12.7-cm NIST traceable radiance calibration panel. This prevents fluctuating downwelling irradiance from saturating the detector.

Raw reflectance spectra were processed using R version 2.11.0 (R Development Core Team, 2008) with custom R routines following Chakraborty et al. (2015). These routines involved (i) a parabolic splice to correct for "gaps" between detectors, (ii) averaging replicate spectra, and (iii) fitting a weighted (inverse measurement variance) smoothing spline to each spectrum, with direct extraction of smoothed reflectance at 10-nm intervals. The present study used Savitzky–Golay first-derivative spectra with a first-order polynomial across a 10-band window for subsequent spectral analysis. Mathematical pretreatment of the spectra reduced model error, with pretreatment transformation implemented in the UnscramblerX 10.3 software (CAMO Software Inc.).

Development of Hypothetical Discontinuity Indices

A soil horizon is a layer of soil or soil material approximately parallel to the land surface and differing from adjacent genetically related layers in physical, chemical, and biological properties or characteristics such as color, structure, texture, consistency, kinds and number of organisms present, or degree of acidity or alkalinity (Soil Science Society of America, 2014). The differentiation of soil horizons is critical for the understanding and classification of soil because horizon formation is a function of a variety of physical, chemical, geological, and biological processes associated with the landscape and climate over long time periods (Soil Survey Staff, 1993, 1999; Schaetzl and Thompson, 2015). The process of field horizonation is, to some extent, a subjective approximation of soil features by field soil scientists. Soil scientists use all the tools available to differentiate soil horizons and establish minimal within-horizon variability, considering a variety of soil properties simultaneously. As such, significant variations in soil properties should occur between horizons in a given pedon. Obviously, the most important part of horizonation is the identification of differences between soil horizons (i.e., what makes a given horizon sufficiently different from adjacent horizons above or below, justifying its differentiation as a unique horizon?). As such, for purposes of this research, three different discontinuity indices (differences in laboratory analyses, PXRF-determined elements, and VisNIR-determined spectra) were used as quantitative metrics for differentiating one soil horizon from another.

In this study, we followed the general methodology set forth by Weindorf et al. (2012b), here summarized as follows. Principal component analysis (PCA) was used to establish the degree of horizon differentiation using data collected from scanning layers and various other soil variables as the key components of the data matrix. Essentially, orthogonal transformation was utilized in PCA to change a set of observations of possibly correlated variables into linearly uncorrelated variables known as *principal components* (PCs). Jolliffe (1986) noted that doing so diminishes the chance that correlated variables are continually considered in variance calculations. This procedure results in the establishment of new coordinates, termed *loadings*, to represent the principal component data set variances.

In the present study, pH, EC, fractions of sand, silt, and clay, and SOM were determined for each depth of each pedon; the data from such analyses were then used for PCA. For each evaluated depth, the principal components of the laboratory analysis results were extracted in the matrix of correlation utilizing a minimum retained eigenvalue of 1, 25 maximum iterations, and a convergence level of 0.001, again following Weindorf et al. (2012b). The differences in laboratory analysis (DLAs) between soil layers were established via PCA (Weindorf et al., 2012b):

$$\text{DLA}_n = \sqrt{\sum_{i=1}^{F} \left(L_{i(n-1)} - L_{in} \right)^2} \qquad [1]$$

where DLA_n represents the difference in laboratory analyses of layer n to the layer above, $n - 1$; F is the total number of significant principal components obtained in the PCA; and $L_{i(n-1)}$ and L_{in} are the PC scores of layers n and $n - 1$ on the ith principal component, respectively.

As Weindorf et al. (2012b) noted, because scaling of variables directly impacts PCA, the original laboratory data can be standardized into the same scale for each pedon as divided by the averages of the variables before PCA. Because the original soil property data were placed into the same scale and the principal components routinely accounted for 90% of the variances observed, the differences between data points of the principal components represents the variability of the original data set. As such, when any soil variable is considered, the calculated difference increases accordingly.

As mentioned above, a range of soil features is generally used by field surveyors during the process of horizon description, including soil color, texture, and structure, which are essentially affected by the physical and chemical composition of the soil. For example, besides SOM and water content, Fe and Mn are the primary coloring agents for many soils. Several soil variables including pH, silt/clay fraction, SOM, oxides and hydroxides, and microorganisms are documented as factors influencing the content and behavior of trace elements (Kabata-Pendias and Pendias, 2001). While elemental variability has not traditionally been used for horizon differentiation, it represents quantifiable chemical differences within the soil and a viable parameter for unique horizon recognition. Portable X-ray fluorescence scanning provides quantifiable data on a large number of macro

and trace elements. Thus, the abundance of a single element or several elements within a given pedon can be considered jointly with other factors when assigning horizon boundaries. As such, differences of elements (DEs), as determined by PXRF, between horizons were calculated (Weindorf et al., 2012b):

$$\text{DE}_n = \sqrt{\sum_{i=1}^{F} \left(L_{i(n-1)} - L_{in} \right)^2} \qquad [2]$$

where DE_n is the difference of elemental contents of the layer n to the layer above, $n - 1$. Likewise, changes in elemental abundance within the pedon cause an increase in the DEs between soil layers. Considering both the elemental precision level of the PXRF and the elemental ranges found by PXRF within the profiles, the contents of 15 elements (K, Ca, Ti, V, Cr, Mn, Fe, Ni, Cu, Zn, Rb, Sr, Zr, Ba, and Pb) were selected for PCA in this study, but only elements with a measured quantity more than 10 times greater than their reported PXRF errors were selected for use.

Finally, in the same manner, the calculated differences (CDs) of VisNIR DRS reflectance values between soil layers were established via PCA (adapted from Weindorf et al., 2012b):

$$\text{VisNIR differences}_n = \sqrt{\sum_{i=1}^{F} \left(L_{i(n-1)} - L_{in} \right)^2} \quad [3]$$

Equations [2] and [3] are fundamentally the same as Eq. [1], except the PXRF readings of elemental contents and VisNIR DRS reflectance values were used as the matrix for PCA in Eq. [2] and [3], respectively. Notably, because SOM is a key factor in horizon differentiation, we considered only a subset (1700–2500 nm) of the total VisNIR DRS range, which has been proven as the most informative region for SOM (Sudduth and Hummel, 1993). All statistical analyses were executed in XL Stat 2014 (Addinsoft).

RESULTS AND DISCUSSION
Field and Laboratory Assessment

Results of our laboratory analyses are presented in Supplementary Table S1. Analyses of some samples from Italy and Hungary were not possible due to the limited sample quantity available after shipment.

Texas

Most of the Texas soils had sandy soil textures, often sandy loam. Site TX-1 consisted of shallow playa lacustrine sediments with overlying sandy aeolian sediments, thus establishing the lithologic discontinuity. Laboratory data showed a doubling of SOM concentration at a depth of 30 to 40 cm (1.00%) vs. the overlying horizon (0.50%). Similarly, clay content increased from 22 to 35% at that boundary, causing soil texture to shift from sandy clay loam to sandy clay. However, an even more pronounced shift in soil properties was observed at a depth of 60 to 70 cm, where clay content increased dramatically (42%) relative to the overlying horizon (28%); the textural class of the former is clay while the latter is sandy clay loam. Such laboratory data align well with field morphological evidence of a discontinuity,

only one of which was noted in situ at 55 cm (Supplementary Table S1).

By contrast, field investigation identified two possible discontinuities at Site TX-2 (at depths of 33 and 77 cm). The soil was mapped as an Amarillo fine sandy loam, which is often buried to various thicknesses by soil material that has eroded by wind from the adjacent dunes mantled by Drake soils (Aridic Calciustepts). Laboratory data supported the two suspected discontinuities owing to a doubling of SOM (0.20 to 0.51%) at 33 cm and an abrupt reduction at 77 cm (0.52 to 0.18%). Similarly, at these same depths, clay content changed from 17 to 28 and 36 to 23%, respectively.

Site TX-3 consisted of a Quaternary alluvial sandy loam soil in a shallow draw covered by aeolian influence from Midessa (Aridic Calciustept) and Posey (Calcidic Paleustalf) sandy loam soils in surrounding upland positions (Soil Survey Staff, 2015). While similar taxonomically, Drake and Midessa soils differ in their $CaCO_3$ equivalent in calcic horizons, the former having <40% (Soil Survey Staff, 2015). In situ evaluation of the pedon suggested a discontinuity at 90 cm. Laboratory data detected physicochemical differences at the same depth but also a smaller possible discontinuity at 50 cm reflected by a sudden doubling of SOM (0.15 to 0.34%) and modest increases in EC and clay content relative to overlying horizons, all of which showed steady decreases. However, laboratory data showed that the lower discontinuity boundary would be more aptly placed at 100 cm, where differences in SOM and clay were more apparent. It is fair to note that many of the parameters evaluated as part of this study have the ability to translocate within a given soil profile (e.g., clay, SOM, salts, $CaCO_3$). However, such translocation tends to decrease rapidly with depth in areas under moisture-limited semiarid climates.

Site TX-4 was in a low topographic position, with sand and sandy loam soil but with surficial inputs from soil material derived from Tokio (Calcidic Haplustalf) sandy loam soil in somewhat higher topographic positions (Soil Survey Staff, 2015). Similar to TX-3, the depth of the discontinuity noted in situ could be adjusted downward by ~15 cm to correspond with laboratory data. An in situ discontinuity depth of 35 cm was proposed, but laboratory data showed pronounced, abrupt differences in physicochemical properties at 50 cm, where SOM doubled, $CaCO_3$ doubled, clay increased 10%, and texture shifted from loamy sand to sandy clay loam. Notably, some translocated materials within a given soil profile may be deposited above or below the actual discontinuity owing to differential hydraulic conductivity affected by shifting soil texture or other factors. For example, Weindorf et al. (2010) discussed the impact of hydraulic discontinuity on the formation of placic horizons in Louisiana. Thus, the location of the actual discontinuity must be considered carefully in the context of accumulations or physicochemical differentia that may occur either slightly above or below the actual LD.

Site TX-5 was similar to TX-3, featuring aeolian deposits of sandy loam soil with inputs from nearby Midessa and Tokio soils. Here, the laboratory data supported discontinuity establishment

in the same location as the in situ morphological assessment (52 cm) (Supplementary Table S1). At this depth, SOM increased by 1.5-fold, clay content doubled, and increases in salinity and $CaCO_3$ were observed relative to overlying horizons. While many of these features may initially be considered part of normal subsoil pedogenesis through illuvial processes, the compelling parameter is the SOM concentration. Subsoil increases in SOM alone may lead evaluators to consider this as a buried soil. However, when considered simultaneously with other physicochemical factors showing pronounced differences, lithologic discontinuity recognition is reasonable, possibly in conjunction with being buried.

Italy

Pedon IT-2 (Valleremita) occurred on a very steep, forested hillslope (~55% slope) and featured multiple discontinuities as colluvium from differential sources. Morphological field description indicated discontinuities at 61, 86, 116, and 143 cm. Laboratory data were variable across horizons, with some trends noted, although not as obviously as some other pedons. Specifically, there was a trend of decreasing SOM from the surface (18.12%) to a depth of 90 to 100 cm (0.66%)—a boundary that probably coincides with the second suspected discontinuity at 86 cm. Soil organic matter increased again to a depth of 130 to 140 cm (2.46%), coinciding with the fourth suspected discontinuity. Less profound differences were observed at 61 cm, with sand and silt contents increasing 3 to 4% while clay content decreased by 7%. Few remarkable changes were detected in the laboratory data at 116 cm, suggesting that the field notation may be in error (a suggestion later refuted by proximally sensed data).

In situ, Pedon IT-3 (Gallignano) was suspected of having a discontinuity at 41 cm as colluvium over residuum. However, laboratory data not only discounted this suspected discontinuity, they identified a likely alternate deeper in the profile. While no remarkable differences in laboratory data were noted at 41 cm, laboratory data indicated a clear shift at 110 to 120 cm where, relative to the overlying horizon, the texture shifted from loam to sandy loam, sand content increased 21%, silt content decreased 15%, and SOM dipped to 0.25% (the lowest in the entire profile) before increasing again with the next lower horizon. This one single depth (110–120 cm) also represented the highest salinity (352 $\mu S\ m^{-1}$) of any depth below 30 cm.

Hungary

Three pedons were evaluated in Hungary, each showing differential expression of possible discontinuities. In situ, Pedon HU-2 showed a strong calcic horizon at 100 cm, an area where a suspected discontinuity occurred. However, high levels of $CaCO_3$ accumulation may also have been due to normal pedogenesis, casting doubt on this initial supposition. Laboratory data clearly showed a doubling of C (1.3 to 2.9%) at the 100-cm boundary. Also, clay content decreased ~4% relative to the overlying horizon—a modest decrease, but one that also changes the soil textural class from silty clay loam to silt loam. Interestingly,

at the 110- to 120-cm depth, SOM reached a minimum of 0.58% before steadily increasing below that with depth. Thus, the increase in SOM deep in the profile gives an indication that a discontinuity in this area may be warranted as opposed to simple pedogenic carbonate accumulation.

In situ evaluation of Pedon HU-4 indicated two possible discontinuities: 90 and 146 cm (loess over lacustrine sediments). Both suspected discontinuities were clearly observable in the laboratory data. Relative to the overlying horizon, the SOM doubled (0.32 to 0.60%) and EC tripled (107 to 382 μS m^{-1}) at 90 cm. At 140 to 150 cm, sand content decreased by 22%, silt content increased by 16%, and C content went from 2.35 to 4.07% relative to the overlying horizon. A third discontinuity was clearly evident in the laboratory data, although elusive during field description. At 110 to 120 cm, the soil texture was silt loam and C was 6.30%. Both overlying and underlying horizons were sandy loam, while the C content was 0.34% above and 3.89% below.

Pedon HU-5 showed evidence of a discontinuity at 80 cm in situ. Although debatable as to the exact depth at which the discontinuity started, laboratory data clearly showed a dramatic shift in physicochemical properties from 80 to 110 cm. Except for the surface horizon (probably impacted by soil pit spoil), the upper part of the profile was acidic (4.1–4.8) and showed a steady increase in clay content from sandy loam (14% clay), to sandy clay loam (23–31% clay), to clay (40% clay) with depth. At 90 cm, however, the clay content began to decrease, silt content began to increase, and C levels increased by as much as 20-fold. While the silt content can be linked to calcic horizon formation, this does not explain the rapid decrease in sand content (68% in the upper part of the profile, decreasing to 22% by 100 cm). At 80 to 90 cm, SOM was also the highest of any horizon (0.91%) in this profile except for the surface horizon. As such, discontinuity status in this profile is likely.

Proximal Sensor Approaches

In discussing the ability of PXRF and VisNIR DRS to elucidate differences in profile parent material origin, the 10 evaluated pedons were qualitatively grouped into classes of good, fair, and poor for both PXRF and VisNIR DRS. Notably, these classes were comparing the field-determined LDs with PXRF and VisNIR data. Often, laboratory characterization data were useful in helping to explain why PXRF and VisNIR data plots performed the way they did in Fig. 2, 3, and 4. "Good" matches between the data sets indicated that proximal sensor data aligned well with field-described LDs; that is, plot maxima and minima generally occurred within ~5 cm of the field-described discontinuity, with most discontinuities within a given pedon meeting this criterion. "Fair" matches between the data sets indicated that proximal sensor data somewhat aligned with field-described LDs. For example, the data sets identified LDs at approximately the same depths, but proximal sensor data suggested that a given LD might be more appropriately placed 10 to 20 cm higher or lower than the field-described LDs. Furthermore, "fair" matches

could contain a mix of multiple LD plot alignments, some of which were "good" while others were "poor." "Poor" matches between the data sets indicated almost no relation between field-described LDs and proximal sensor data. Often, this was expressed as nondescript plots with no maxima or minima, or plots where field-described LDs were >20 to 30 cm from proximal sensor maxima or minima. In some instances, laboratory data and/or field-suspected discontinuities aligned with PXRF and VisNIR DRS predictive plots. But in other instances, wide discrepancy was found. Weindorf et al. (2012b, 2014) outlined the rationale for such differences with regard to PXRF as follows: (i) PXRF data align well with traditional morphological horizons, (ii) PXRF reveals more horizons than traditional morphological descriptions due to differences in elemental concentrations imperceptible to the human eye, and/or (iii) PXRF reveals fewer horizons than morphological descriptions based on differences undetectable to the PXRF (e.g., differences in soil structure, rooting, bulk density, soil organic C). Although VisNIR DRS should reasonably be able to detect differences in organic C (Morgan et al., 2009) (and by extension perhaps even differences in rooting density), soil characteristics such as bulk density, soil structure, and consistence probably remain elusive to these two proximal sensors. However, those characteristics seldom form the sole basis for LD designation. Nonetheless, we do not advocate the sole use of proximal sensors for LD establishment. Rather, we suggest that such sensors can provide useful quantitative elemental and spectral data that can be used to complement traditional morphological description, especially in instances where the boundaries of LDs are morphologically nondescript.

PXRF Assessment

With regard to PXRF analysis of discontinuity assessment, eight pedons qualitatively showed good alignment with laboratory- and/or field-established discontinuities; two pedons were fair. In most instances, PXRF discontinuities were marked by either maximum or minimum DE values evaluated on a pedon by pedon basis (Fig. 2). In some cases, these maximum and minimum values were helpful in adjusting the depth of the laboratory- or field-determined discontinuity where clear trends were observed.

Pedons TX-1 and TX-2 showed fair alignment, while TX-3, TX-4, and TX-5 showed good alignment. In TX-1, the field-suspected discontinuity at 55 cm was nondetectable by PXRF; these results were supported by laboratory data. However, laboratory data pointed to a discontinuity at 60 to 70 cm, and at 70 cm, PXRF DEs reached a minimum, suggesting a possible discontinuity. At TX-2, a field-suspected discontinuity at 33 cm aligned well with a PXRF DE maximum and laboratory data. However, the second field-suspected discontinuity at 77 cm was not well represented by PXRF DEs. Here, the DE trend line was moving steadily downward but not near a maximum or minimum value. As such, the PXRF DE minimum was not achieved until 90 cm, a considerable departure from laboratory and field data. However, laboratory data aligned well with the PXRF DE
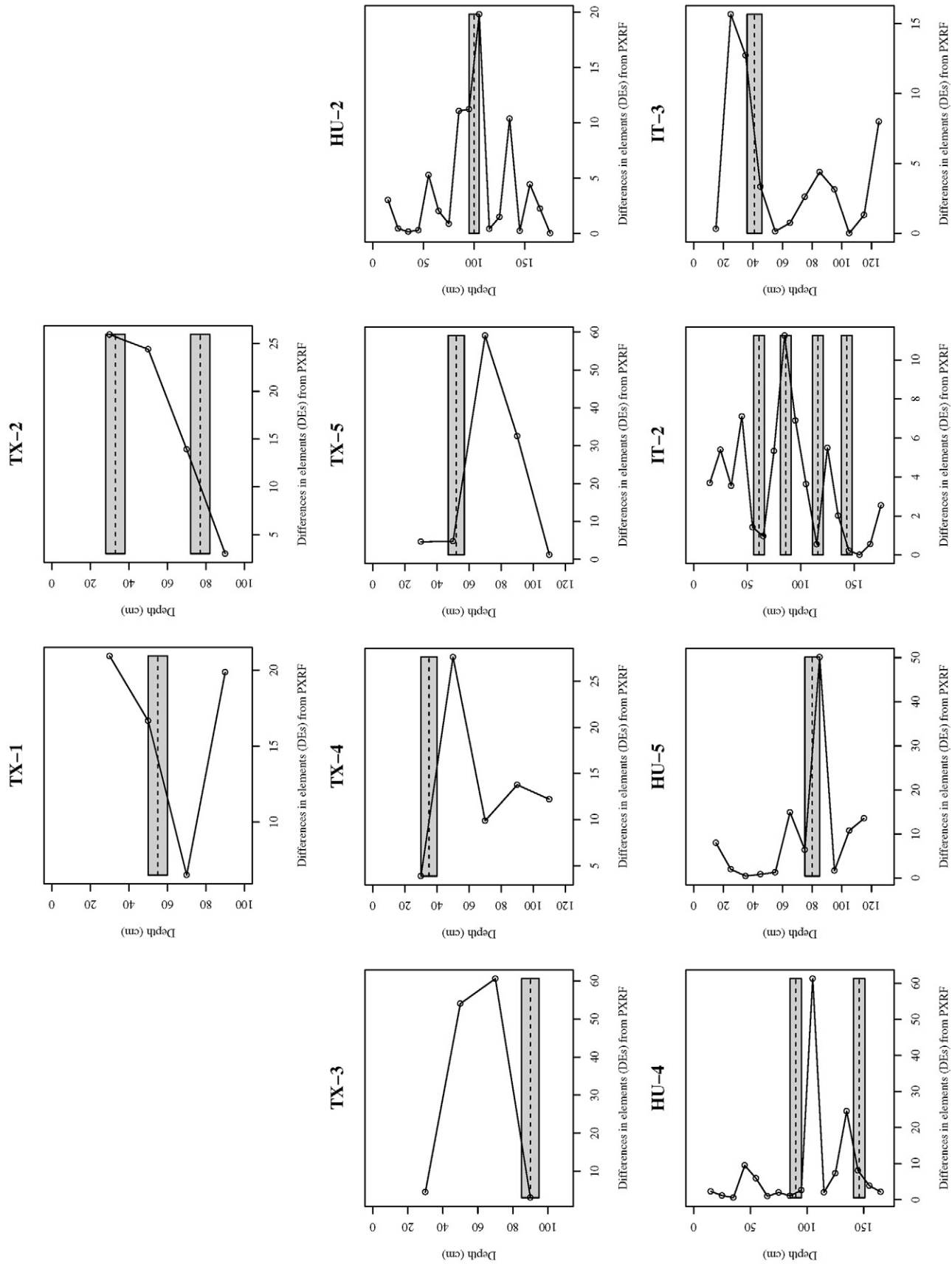
Fig. 2. Differences of element (DEs) as determined by portable X-ray fluorescence spectrometry for 10 pedons suspected of having lithologic discontinuities in Texas, Italy, and Hungary. Field-suspected discontinuity depths are noted with a dashed line bounded by a gray bar of ±5 cm.

minimum at 90 cm, showing maximum sand content, minimum clay content, and minimum subsoil SOM at this same depth (Fig. 3) and suggesting that the field-identified discontinuity might be more aptly lowered from 77 to 90 cm. The remaining Texas pedons showed strong alignment between PXRF and laboratory and field discontinuity locations. At TX-3, a minimum PXRF DE was found at 90 cm, very near the field and laboratory suspected discontinuity. Portable X-ray fluorescence provides some support for evaluating a possible second discontinuity at ~60 cm, where laboratory data showed some indications of a discontinuity and PXRF DEs were maximized. At TX-4, the PXRF DE minimum at 30 cm aligned well with a field discontinuity suspected at 35 cm, and a laboratory-suspected discontinuity at 50 cm was reflected strongly by a PXRF DE maximum at that same depth. Finally, a PXRF minimum DE at 52 cm in TX-5 aligned well with both laboratory and field data in support of a discontinuity at that depth.

Of all the pedons evaluated, Pedon IT-2 was the most complex, with four different field-suspected discontinuities. Somewhat surprisingly, PXRF did an excellent job at noting these, showing wide swings in DE maxima and minima accordingly. Field-suspected discontinuities were set at 61, 86, 116, and 143 cm. At 60 to 70 cm, PXRF DEs were minimum, but by 80 to 90 cm they had shifted to maximum, aligning perfectly with both field and laboratory data. At 116 cm, laboratory data were marginal in supporting a field-suspected discontinuity, but PXRF reached a DE minimum in perfect unison with the field depth. For the lowest discontinuity, laboratory data suggested that moving the depth slightly higher in the profile might be appropriate. However, a PXRF DE minimum suggested that the field assessment was accurate and should be left unchanged. For Pedon IT-3, PXRF data indicated that the suspected field discontinuity at 41 cm should be moved slightly higher in the profile, as a DE maximum was achieved at ~25 cm. Although not noted in the field, a suspected laboratory-identified discontinuity at ~110 to 120 cm was well supported by a PXRF DE minimum achieved at that same depth. Here, both laboratory data and PXRF were compelling in identifying something different in the soil substrate that was not visually detectable.

All three Hungarian pedons showed good alignment between PXRF and laboratory and field data. Pedon HU-2 had a field-suspected discontinuity at 100 cm. However, laboratory data suggested that it would be more appropriately moved deeper to 110 to 120 cm (noted by the green dashed line in Fig. 3). A PXRF DE minimum was reached at ~115 cm, a depth at which maximum silt, minimum clay, and near-minimum subsoil SOM levels were achieved (Fig. 3). Pedon HU-4 had field-suspected discontinuities at 90 and 146 cm. The former was well captured by a PXRF DE minimum, while the latter was not well captured by PXRF; the DE trend line was still decreasing at that depth. While not evident in the field, laboratory data showed a possible discontinuity at 110 to 120 cm, a depth clearly captured by a PXRF DE maximum at ~110 cm. Finally, Pedon HU-5 showed a maximum PXRF DE at ~83 cm, clearly reflective of both labo-
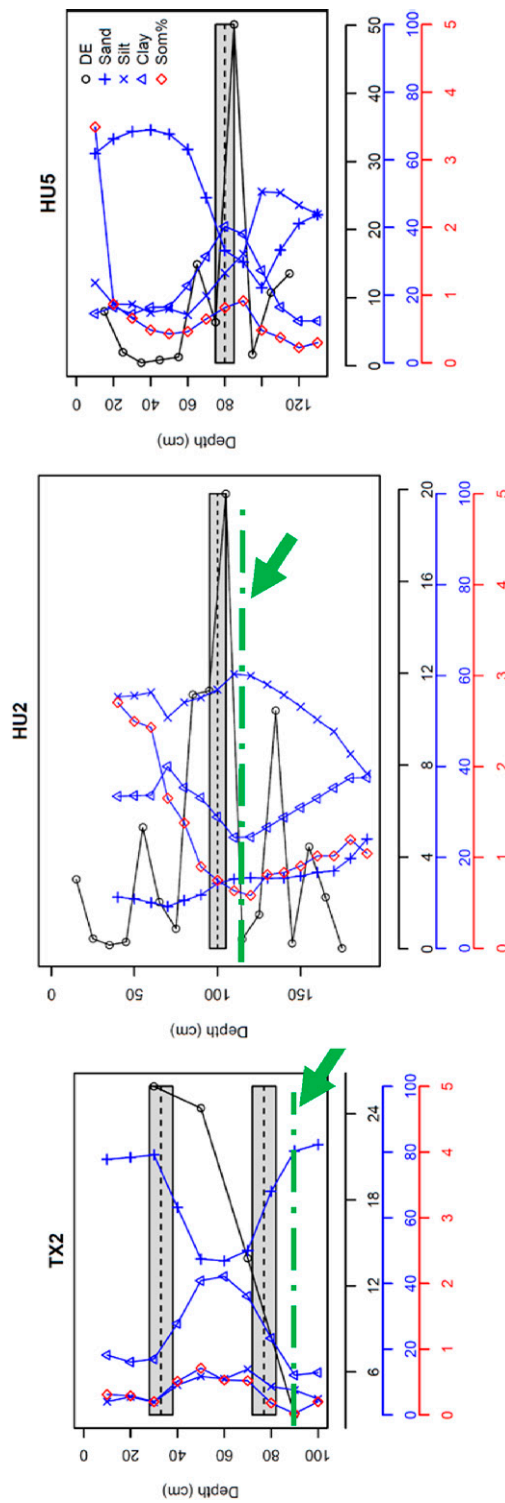
Fig. 3. Depth plots showing the differences of elements (DEs) as determined by portable X-ray fluorescence (PXRF) spectrometry against laboratory-determined characterization data (sand, silt, clay, and soil organic matter [SOM] percentages) and morphologically established discontinuities (gray shaded boxes) for Pedons TX-2 from Texas and HU-2 and HU-5 from Hungary. Pedon HU-5 is an example of good alignment among proximal data, field morphological assessment, and laboratory data, while Pedons TX-2 and HU-2 are examples of PXRF DE minima suggesting that the morphologically established discontinuity should probably be recognized ~15 cm deeper in the profile where PXRF data and laboratory data closely align (noted by green dashed line).

ratory and field discontinuity placement at 80 cm. Here, the clay reached a maximum and subsoil SOM was near its maximum as well; both declined sharply below this depth.

The plots shown in Fig. 3 lead to an important question: should morphological or laboratory-based data take precedence in assigning a discontinuity in soils? While both are important, the physicochemical laboratory-based data are often elevated in stature owing to their quantitative limits rather than qualitative measures used by morphological description. If nothing else, this research has illustrated instances where laboratory and morphological data do not precisely align in establishing discontinuities. However, PXRF has repeatedly shown a propensity to reflect quantitative differences in soil physicochemical properties as illustrated by laboratory characterization data.

VisNIR DRS Assessment

For VisNIR DRS analysis of discontinuity assessment, five pedons qualitatively showed good alignment with laboratory- and/or field-established discontinuities, three pedons were fair, and two were poor. Similar to the PXRF DE differential, VisNIR DRS-identified discontinuities were marked by either maxima or minima in calculated spectral differences (Fig. 4). Recall that VisNIR DRS is especially sensitive to organic C within soils; thus, deference will be paid to how calculated differences (CDs) aligned with SOM content.

The Texas pedons were among the weakest in showing VisNIR DRS-indicated discontinuities, with one good, two fair, and two poor results. Pedon TX-1 showed a decreased CD at the suspected field discontinuity (55 cm), qualifying it for fair matching, but it did not align well with maximum and minimum CDs in the pedon. Even worse, TX-2 field-suspected discontinuities occurred on actively sloped CDs, again not reflective of CD maxima and minima. Pedon TX-3 was the best of the Texas pedons, with a CD minimum at ∼85 to 95 cm, aligning nicely with a field-identified discontinuity at 90 cm. Pedon TX-4 had a near-minimum CD at 35 cm, but VisNIR DRS data showed that it might be more appropriately placed slightly deeper at ∼45 cm. At this same depth, a PXRF DE maximum further supported the idea of abrupt changes in soil properties at this depth. A possible discontinuity in Pedon TX-5 was among the worst identified by VisNIR DRS. While PXRF was highly capable of noting changes in the profile at 55 cm, VisNIR DRS showed a broad, low CD spread with no remarkable spikes at that depth. A large CD peak was noted at ∼100 cm, probably reflecting the ∼5 to 10% increase in $CaCO_3$ present at that depth relative to the underlying and overlying horizons, which should logically affect spectral reflectance as a feature of color. However, other laboratory data were unremarkable at this depth and the increase in $CaCO_3$ is probably simply pedogenic.

The Italian pedons were among the best characterized by VisNIR DRS. Pedon IT-2 had clear and compelling CD maxima and minima at each of the field-identified discontinuities. Similarly, Pedon IT-3 reached a CD minimum at ∼45 cm, aligning nicely with the field-identified discontinuity. Furthermore, a

laboratory-suspected discontinuity at ∼115 cm was well identified in the VisNIR DRS data as a CD maximum.

The Hungarian pedons were generally well described by VisNIR DRS, with two pedons showing good and one showing fair alignment with field-identified discontinuities. For Pedon HU-2, a field-suspected discontinuity at 100 cm was clearly marked by a CD minimum in the VisNIR DRS data. Pedon HU-4 was fair in its assessment, showing a clear CD minimum at one field discontinuity (90 cm) but rather unremarkable CD features at the second field discontinuity (146 cm). Somewhat surprisingly, one of the compelling features of the second discontinuity was a sharp increase in organic C, yet VisNIR DRS seemed unable to capture this in the subsoil pedon CD. Pedon HU-5 showed better alignment, with a VisNIR DRS CD minimum aligning well with a field-described discontinuity at 80 cm.

Application of VisNIR DRS and PXRF in Discontinuity Evaluation

In conducting this research, PXRF was noted to be slightly better at discontinuity assessment than VisNIR DRS (Table 2). Shifts in soil mineralogical composition are more likely to be adeptly quantified as elemental differences rather than alterations in reflectance spectra. This is not to say that reflectance spectra are useless in this regard; rather, both techniques can be used as complimentary approaches. In some instances, VisNIR DRS will have capabilities to sense differential levels of organic C in soils—a parameter imperceptible to PXRF directly. In other instances, PXRF and VisNIR DRS can dualistically elucidate differences in a soil profile. For example, in areas with a pronounced calcic horizon, PXRF will sense higher levels of Ca, while VisNIR DRS will detect greater spectral reflectance owing to a lighter soil color. What remains to be interpreted by the analyst is whether such differences represent natural pedogenic accumulations (e.g., illuviated clay, $CACO_3$, gypsum) or a true indicator of a lithologic discontinuity. In fact, one important parameter to be considered is whether the soils being evaluated should be classified as buried soils. In this case, the irregular decrease in organic C with depth (Soil Survey Staff, 2014b) should be considered more strongly than other factors, for example for alluvial soils subject to flooding in low-lying areas.

One of the more important conclusions identified by the present study is the concept that relative maxima and minima in either DEs or CDs of PXRF or VisNIR DRS data, respectively, can be important indicators of possible changes in soil parent material. In some instances, these depths are easily reflected in traditional morphological description or laboratory data, but in other areas, they are less visually remarkable. In essence, the maxima and minima for the proximal sensors presented here provide analysts with ancillary information that can warrant more careful evaluation of certain depths or boundaries within the soil, whether visually perceptible or not.

In summary, we conclude that the data afforded by the use of PXRF and VisNIR DRS offer pedologists unique insights into predicted differences between soil horizons—differences
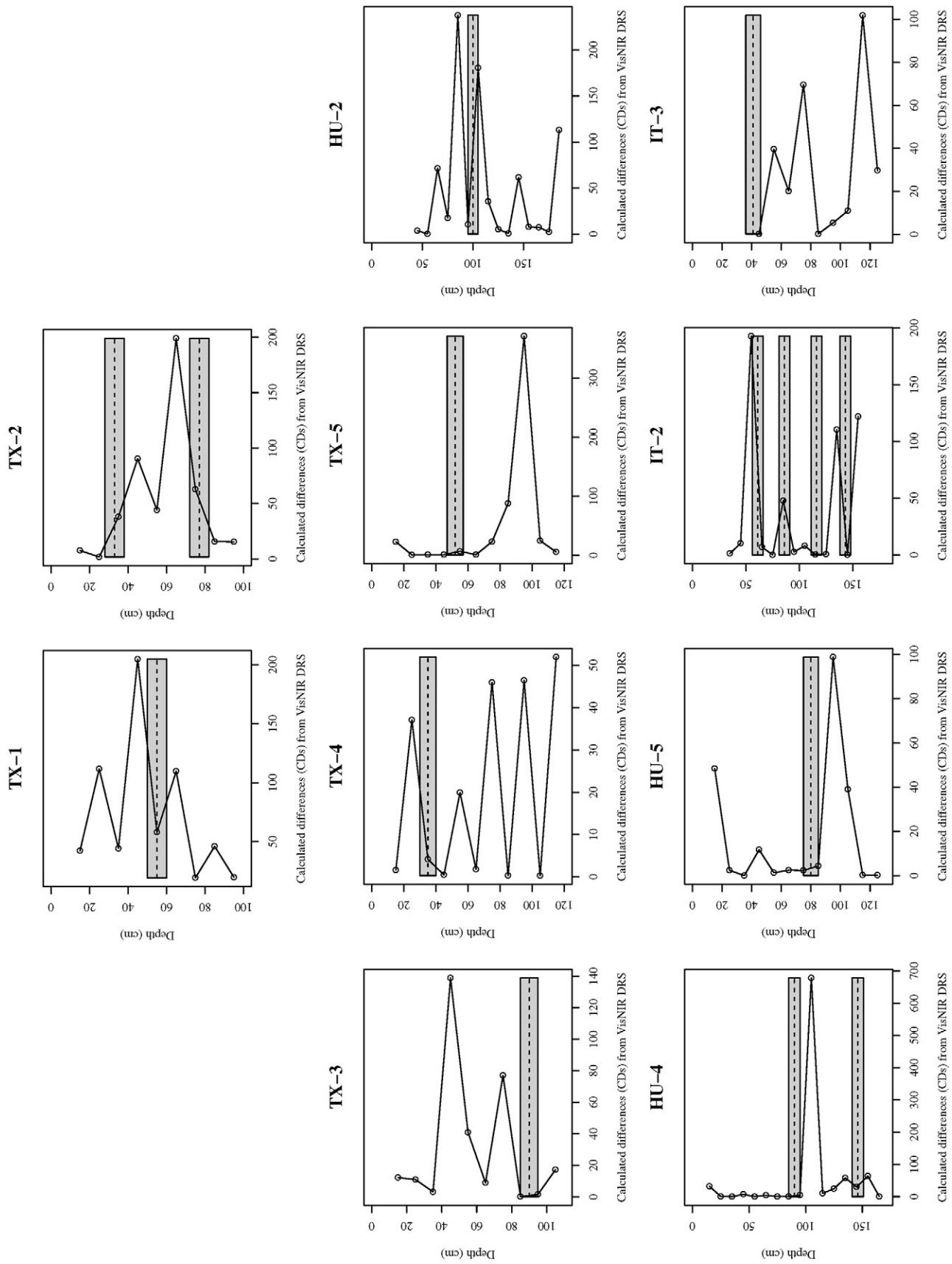
Fig. 4. Calculated differences (CDs) of visible near-infrared diffuse reflectance spectroscopy reflectance values between soil layers for 10 pedons suspected of having lithologic discontinuities in Texas, Italy, and Hungary. Field-suspected discontinuity depths are noted with a dashed line bounded by a gray bar of ±5 cm.

Table 2. Summary of qualitative alignment of portable X-ray fluorescence (PXRF) spectroscopy and visible near infrared diffuse reflectance spectrometry (VisNIR DRS) with field suspected lithologic discontinuities in Texas, Italy, and Hungary.

Pedon	PXRF	VisNIR DRS
TX-1	fair	fair
TX-2	fair	poor
TX-3	good	good
TX-4	good	fair
TX-5	good	poor
IT-2	good	good
IT-3	good	good
HU-2	good	good
HU-4	good	fair
HU-5	good	good
	Total (*n*)	
Good	8	5
Fair	2	3
Poor	0	2

that may be indicative of lithologic discontinuities. We do not advocate the strict use of proximal sensors in the establishment of discontinuities, absent laboratory and morphological data. However, these instruments provide pedologists with another data stream, quickly and easily acquired in situ, that can help identify areas of lithologic discontinuity within a given pedon, whether visually observable or not. Collectively, these proximal sensors can detect depth changes in both organic and inorganic soil constituents, many of which may align with changes in parent material. Hence, the method may offer insight into the presence of discontinuities that may not normally have been detected in the field.

CONCLUSIONS

This research evaluated the use of PXRF spectrometry and VisNIR DRS for identification of lithologic discontinuities in soils. Ten pedons consisting of 135 sampled depths from three different countries were scanned with both proximal sensors, and the data were then compared with both standard laboratory-generated soil characterization data as well as morphological descriptive data noted in situ. Results showed that large, abrupt changes in standardized PXRF DEs often successfully identified discontinuities (whether suggested by laboratory data or morphological description) appearing in the data plots as DE maxima and minima. Similarly, standardized VisNIR DRS CDs in reflectance spectra (350–2500 nm) identified discontinuities based on CD reflectance maxima and minima. With both types of data plots, discontinuities were not well captured by the proximal sensors when CD or DE values fell in the data plot midsection. Across the 10 pedons evaluated, PXRF appeared to show slightly better detection of discontinuities relative to VisNIR DRS. However, VisNIR DRS also showed dexterity in identifying differences in certain pedons not well captured by PXRF. We recommend the integrated use of proximal sensors in conjunction with laboratory data and morphological evaluation of lithologic discontinuities in soil profiles.

The proximal data are quickly and easily acquired in situ and can provide quantitative differentia in support of discontinuity recognition both in instances where morphological and laboratory data indicate differences but also in instances where differences are morphologically nondescript.

REFERENCES

Aldabaa, A.A.A., D.C. Weindorf, S. Chakraborty, A. Sharma, and B. Li. 2015. Combination of proximal and remote sensing methods for rapid soil salinity quantification. Geoderma 239–240:34–46. doi:10.1016/j.geoderma.2014.09.011

Chakraborty, S., D.C. Weindorf, N. Ali, B. Li, Y. Ge, and J.L. Darilek. 2013. Spectral data mining for rapid measurement of organic matter in unsieved moist compost. Appl. Opt. 52:B82–B92. doi:10.1364/AO.52.000B82

Chakraborty, S., D.C. Weindorf, B. Li, A.A.A. Aldabaa, and M.N. Ali. 2015. Development of a hybrid proximal sensing method for rapid identification of petroleum contaminated soils. Sci. Total Environ. 514:399–408. doi:10.1016/j.scitotenv.2015.01.087

Chakraborty, S., D.C. Weindorf, C.L.S. Morgan, Y. Ge, J.M. Galbraith, B. Li, and C.S. Kahlon. 2010. Rapid identification of oil-contaminated soils using visible near-infrared diffuse reflectance spectroscopy. J. Environ. Qual. 39:1378–1387. doi:10.2134/jeq2010.0183

Foss, J.E., and R.H. Rust. 1968. Soil genesis study of a lithologic discontinuity in glacial drift in western Wisconsin. Soil Sci. Soc. Am. J. 32:393–398. doi:10.2136/sssaj1968.03615995003200030036x

Gee, G.W., and J.W. Bauder. 1986. Particle-size analysis. In: A. Klute, editor, Methods of soil analysis. Part 1. Physical and mineralogical methods. 2nd ed. SSSA Book Ser. 5. SSSA and ASA, Madison, WI. p. 383–411. doi:10.2136/sssabookser5.1.2ed.c15

Habecker, M.A., K. McSweeney, and F.W. Madison. 1990. Identification and genesis of fragipans in Ochrepts of north central Wisconsin. Soil Sci. Soc. Am. J. 54:139–146 . doi:10.2136/sssaj1990.03615995005400010022x

Hartemink, A.E., and B. Minasny. 2014. Towards digital soil morphometrics. Geoderma 230–231:305–317. doi:10.1016/j.geoderma.2014.03.008

Horta, A., B. Malone, U. Stockmann, B. Minasny, T.F.A. Bishop, A.B. McBratney, et al. 2015. Potential of integrated field spectroscopy and spatial analysis for enhanced assessment of soil contamination: A prospective review. Geoderma 241–242:180–209. doi:10.1016/j.geoderma.2014.11.024

Horváth, E. 2001. Marker horizons in the loesses of the Carpathian Basin. Quat. Int. 76–77:157–163. doi:10.1016/S1040-6182(00)00099-9

Horváth, Z., E. Michéli, A. Mindszenty, and J. Berényi-Üveges. 2005. Soft-sediment deformation structures in Late Miocene–Pleistocene sediments on the pediment of the Mátra Hills. Tectonophysics 410:81–95. doi:10.1016/j.tecto.2005.08.012

Jolliffe, I.T. 1986. Principal component analysis. Springer-Verlag, New York.

Kabata-Pendias, A., and H. Pendias. 2001. Trace elements in soils and plants. CRC Press, Boca Raton, FL.

McLaren, T.I., C.N. Guppy, M.K. Tighe, N. Forster, P. Grave, L.M. Lisle, and J.W. Bennett. 2012. Rapid, nondestructive total elemental analysis of Vertisol soils using portable X-ray fluorescence. Soil Sci. Soc. Am. J. 76:1436–1445. doi:10.2136/sssaj2011.0354

Melquiades, F.L., R.O. Bastosa, G.E.V. Biasia, P.S. Parreirab, and C.R. Appoloni. 2011. Granulometry and moisture influence for in situ soil analysis by portable EDXRF. In: Proceedings of the 33rd Brazilian Workshop on Nuclear Physics, Compos Do Jordao, Brazil. 7-11 Sept. 2010. AIP Conf. Proc. 1351:317–320.

Michéli, E., M. Fuchs, P. Hegymegi, and P. Stefanovits. 2006. Classification of the major soils of Hungary and their correlation with the World Reference

Base for Soil Resources (WRB). Agrokem. Talajtan 55:19–328.

Morgan, C.L.S., T.H. Waiser, D.J. Brown, and C.T. Hallmark. 2009. Simulated in situ characterization of soil organic and inorganic carbon with visible near-infrared diffuse reflectance spectroscopy. Geoderma 151:249–256. doi:10.1016/j.geoderma.2009.04.010

Nelson, D.W., and L.E. Sommers. 1996. Total carbon, organic carbon, and organic matter. In: D.L. Sparks, editor, Methods of soil analysis. Part 3. SSSA Book Ser. 5. SSSA and ASA, Madison, WI. p. 961–1010. doi:10.2136/sssabookser5.3.c34

Paulette, L., T. Man, D.C. Weindorf, and T. Person. 2015. Rapid assessment of soil and contaminant variability via portable X-ray fluorescence spectroscopy: Copşa Mică, Romania. Geoderma 243–244:130–140. doi:10.1016/j.geoderma.2014.12.025

Phillips, J.D., and C. Lorz. 2008. Origins and implications of soil layering. Earth Sci. Rev. 89:144–155. doi:10.1016/j.earscirev.2008.04.003

Piorek, S. 1998. Determination of metals in soils by field-portable XRF spectrometry. In: V. Lopez-Avila et al., editors, Current protocols in field analytical chemistry. John Wiley & Sons, New York. p. 3B.1.1–3B.1.18.

Price, T.W., R.L. Blevins, R.I. Barnhisel, and H.H. Bailey. 1975. Lithologic discontinuities in loessial soils of southwestern Kentucky. Soil Sci. Soc. Am. J. 39:94–98. doi:10.2136/sssaj1975.03615995003900010026x

R Development Core Team. 2008. R: A language and environment for statistical computing. R Found. Stat. Comput., Vienna. http://www.cran.r-project.org (accessed 6 Jan. 2014).

Raad, A.T., and R. Protz. 1971. A new method for the identification of sediment stratification in soils of the Blue Springs basin. Geoderma 6:23–41. doi:10.1016/0016-7061(71)90049-8

Salinity Laboratory Staff. 1954. Diagnosis and improvement of saline and alkali soils. Agric. Handb. 60. US Gov. Print. Office, Washington, DC.

Schaetzl, R. 1998. Lithologic discontinuities in some soils on drumlins: Theory, detection, and application. Soil Sci. 163:570–590. doi:10.1097/00010694-199807000-00006

Schaetzl, R., and M.D. Luehmann. 2013. Coarse-textured basal zones in thin loess deposits: Products of sediment mixing and/or paleoenvironmental change? Geoderma 192:277–285. doi:10.1016/j.geoderma.2012.08.001

Schaetzl, R., and M.L. Thompson. 2015. Soils: Genesis and geomorphology. 2nd ed. Cambridge Univ. Press, Cambridge, UK.

Schoeneberger, P.J., D.A. Wysocki, E.C. Benham, and W.D. Broderson, editors. 2002. Field book for describing and sampling soils, Version 2.0. Natl. Soil Surv. Ctr., Lincoln, NE.

Sharma, A., D.C. Weindorf, T. Man, A. Aldabaa, and S. Chakraborty. 2014. Characterizing soils via portable X-ray fluorescence spectrometer: 3. Soil reaction (pH). Geoderma 232–234:141–147 . doi:10.1016/j.geoderma.2014.05.005

Sharma, A., D.C. Weindorf, D.D. Wang, and S. Chakraborty. 2015. Characterizing soils via portable X-ray fluorescence spectrometer: 4. Cation exchange capacity (CEC). Geoderma 239–240:130–134 . doi:10.1016/j.geoderma.2014.10.001

Sherrod, L.A., G. Dunn, G.A. Peterson, and R.L. Kolberg. 2002. Inorganic carbon analysis by modified pressure-calcimeter method. Soil Sci. Soc. Am. J. 66:299–305. doi:10.2136/sssaj2002.0299

Soil Science Society of America. 2014. Glossary of soil science terms. SSSA, Madison, WI. https://www.soils.org/publications/soils-glossary (accessed 18 June 2014).

Soil Survey Staff. 1993. Soil survey manual. Agric. Handb. 18. US Gov. Print. Office, Washington, DC.

Soil Survey Staff. 1999. Soil taxonomy: A basic system of soil classification for making and interpreting soil surveys. 2nd ed. Agric. Handb. 436. US Gov. Print. Office, Washington, DC.

Soil Survey Staff. 2004. Soil survey laboratory methods manual. U.S. Gov. Print. Office, Washington, DC.

Soil Survey Staff. 2006. Land resource regions and major land resource areas of the United States, the Caribbean, and the Pacific Basin. Agric. Handb. 296. NRCS, Washington, DC. http://www.nrcs.usda.gov/Internet/FSE_DOCUMENTS/nrcs142p2_050898.pdf (accessed 18 June 2014).

Soil Survey Staff. 2010. Keys to Soil Taxonomy. 11th ed. NRCS, Washington, DC.

Soil Survey Staff. 2014a. Soil survey laboratory methods manual. Soil Survey Invest. Rep. 42. Version 5.0. Kellogg Soil Surv. Lab., Lincoln, NE.

Soil Survey Staff. 2014b. Illustrated guide to Soil Taxonomy. Natl. Soil Surv. Ctr., Lincoln, NE.

Soil Survey Staff. 2015. Official soil series descriptions. National Soil Surv. Ctr., Lincoln, NE. https://soilseries.sc.egov.usda.gov/osdname.asp (accessed 17 Feb. 2015).

Stefanovits, P. 1963. The soils of Hungary. 2nd ed. (In Hungarian.) Akadémiai Kiadó, Budapest.

Sudduth, K.A., and J.W. Hummel. 1993. Near-infrared spectrophotometry for soil property sensing. In: J.A. DeShazer and G.E. Meyer, editors, Proceedings of SPIE Conference on Optics in Agriculture and Forestry, Boston, MA. 16–17 Nov. 1992. SPIE Proc. 1836:14–25.

Swanhart, S., D.C. Weindorf, S. Chakraborty, N. Bakr, Y. Zhu, C. Nelson, et al. 2014. Soil salinity measurement via portable X-ray fluorescence spectrometry. Soil Sci. 179:417–423. doi:10.1097/SS.0000000000000088

USEPA. 2007. Method 6200: Field portable X-ray fluorescence spectrometry for the determination of elemental concentrations in soil and sediment. USEPA, Washington, DC. http://www3.epa.gov/epawaste/hazard/testmethods/sw846/pdfs/6200.pdf (accessed 3 Dec. 2013).

Wang, D.D., S. Chakraborty, D.C. Weindorf, B. Li, A. Sharma, S. Paul, and M.N. Ali. 2015. Synthesized proximal sensing for soil characterization: Total carbon and total nitrogen. Geoderma 243–244:157–167. doi:10.1016/j.geoderma.2014.12.011

Weindorf, D.C., N. Bakr, and Y. Zhu. 2014. Advances in portable X-Ray fluorescence (PXRF) for environmental, pedological, and agronomic applications. Adv. Agron. 128:1–45. doi:10.1016/B978-0-12-802139-2.00001-9

Weindorf, D.C., N. Bakr, Y. Zhu, B. Haggard, S. Johnson, and J. Daigle. 2010. Characterization of placic horizons in ironstone soils of Louisiana, USA. Pedosphere 20:409–418. doi:10.1016/S1002-0160(10)60030-6

Weindorf, D.C., J. Herrero, C. Castañeda, N. Bakr, and S. Swanhart. 2013a. Direct soil gypsum quantification via portable X-ray fluorescence spectrometry. Soil Sci. Soc. Am. J. 77:2071–2077. doi:10.2136/sssaj2013.05.0170

Weindorf, D.C., L. Paulette, and T. Man. 2013b. In situ assessment of metal contamination via portable X-ray fluorescence spectroscopy: Zlatna, Romania. Environ. Pollut. 182:92–100. doi:10.1016/j.envpol.2013.07.008

Weindorf, D.C., Y. Zhu, S. Chakraborty, N. Bakr, and B. Huang. 2012a. Use of portable X-ray spectrometry for environmental quality assessment of peri-urban agriculture. Environ. Monit. Assess. 184:217–227. doi:10.1007/s10661-011-1961-6

Weindorf, D.C., Y. Zhu, R. Ferrell, N. Rolong, T. Barnett, B. Allen, et al. 2009. Evaluation of portable X-ray fluorescence for gypsum quantification in soils. Soil Sci. 174:556–562. doi:10.1097/SS.0b013e3181bbbd0b

Weindorf, D.C., Y. Zhu, B. Haggard, J. Lofton, S. Chakraborty, N. Bakr, et al. 2012b. Enhanced pedon horizonation using portable X-ray fluorescence spectroscopy. Soil Sci. Soc. Am. J. 76:522–531. doi:10.2136/sssaj2011.0174

Weindorf, D.C., Y. Zhu, P. McDaniel, M. Valerio, L. Lynn, G. Michaelson, et al. 2012c. Characterizing soils via portable X-ray fluorescence spectrometer: 2. Spodic and albic horizons. Geoderma 189–190:268–277. doi:10.1016/j.geoderma.2012.06.034

Zhu, Y., D.C. Weindorf, S. Chakraborty, B. Haggard, S. Johnson, and N. Bakr. 2010. Characterizing surface soil water with field portable diffuse reflectance spectroscopy. J. Hydrol. 391:133–140. doi:10.1016/j.jhydrol.2010.07.014

Zhu, Y., D.C. Weindorf, and W. Zhang. 2011. Characterizing soils using a portable X-ray fluorescence spectrometer: 1. Soil texture. Geoderma 167–168:167–177. doi:10.1016/j.geoderma.2011.08.010